Interdependence of structural and electrical properties in tantalum/tantalum oxide multilayers

Arnaud Cacucci, Stéphane Loffredo, Valérie Potin, Luc Imhoff, Nicolas Martin

Interdependence of structural and electrical properties in tantalum/tantalum oxide multilayers

Arnaud CACUCCI[(a)], Stéphane LOFFREDO[(a)], Valérie POTIN[(a*)],
Luc IMHOFF[(a)], Nicolas MARTIN[(b)]

[(a)] *Laboratoire Interdisciplinaire Carnot de Bourgogne, UMR 6303 CNRS - Université de Bourgogne, 9, Avenue Alain Savary, BP47870, F-21078 DIJON Cedex, France*
[(b)] *Institut FEMTO-ST, UMR 6174 CNRS, Université de Franche-Comté, ENSMM, UTBM, 32, Avenue de l'observatoire, F-25044, BESANCON Cedex, France*

Abstract

Dc reactive sputtering was used to deposit tantalum metal/oxide periodic nanometric multilayers using the innovative technique namely, the reactive gas pulsing process (RGPP). Different pulsing periods were used for each deposition to produce metal-oxide periodic alternations included between 5 and 80 nm. Structure, crystallinity and chemical composition of these films were systematically investigated by Transmission Electron Microscopy (TEM) and Energy-dispersive X-ray (EDX) spectroscopy techniques. Moreover, electrical properties were also studied by the Van der Pauw technique.

Keywords: Tantalum oxide, thin film, reactive sputtering, gas pulsing, metal, semi-conductor, electricals properties

* Corresponding author. Tel.: +33 3 80 39 59 23; fax: +33 3 80 39 50 69.
E-mail address: valerie.potin@u-bourgogne.fr.

Highlights

Dc reactive sputtering was implemented with the reactive gas pulsing process.

Combination of the structural analyses allowed determining the composition of different phases.

HRTEM pointed out the dependence between electrical properties and nanometric and periodic αTi/fcc-TiO/a-TiO_2 multilayers.

---

1. Introduction

Tantalum oxide compound has great technological interest, particularly because of its optical and electrical performances [1-3]. This kind of material has attracted huge attention in recent years due to its potential applications as high refractive index materials in multilayered interference filters [4], as anti-reflecting coatings for solar cells [5], as optical waveguides [6] and as capacitor dielectric in high density dynamic random access memories (DRAMs) [7-9]. Compared to silicon dioxide, which has a dielectric constant of 3.9, stoichiometric tantalum oxide Ta_2O_5 compounds can provide about 5 to 6 times increase in the capacitance density (dielectric constant of Ta_2O_5 is 20-27). This could lead to a high packing density in the next generations of DRAMs without reducing the thickness of the dielectric materials to unachievable values. Because of such technological attraction, tantalum oxide thin films have been grown by a large variety of deposition methods including anodization, thermal oxidation, ion-assisted deposition, chemical vapour

deposition (CVD) and physical vapour deposition (PVD) [10-15]. The TaO_x films prepared by these different techniques showed widely disperse properties depending on the process parameters, temperature grown, post-annealing conditions, etc. However, the influence of the oxygen concentration on the characteristics of the films has insufficiently been investigated, especially for films prepared by reactive sputtering [16-17]. It mainly comes from the difficulties to synthesize tantalum oxides with tuneable element concentrations due to instabilities of the reactive process [18-20]. Such a drawback restrains the range of reachable chemical compositions and consequently the resulting properties.

The purpose of this paper is to show how structuration of thin multilayers can influence the electrical properties of TaO_x films. The role of the total period Λ and the χ parameter defined as the ratio $\lambda_{met}/\lambda_{ox}$ (where λ_{met} is the thickness of metal sub-layer and λ_{ox} that of the oxide) on the properties of the films is principally investigated. A systematic increase of the oxygen injection time into the pulsing process leads to clear alternation of α-Ta/aTa_2O_5.

2. Materials and methods

Thin films were simultaneously deposited onto (100) silicon wafer and glass substrates by dc reactive magnetron sputtering from a tantalum metallic target (purity 99.6 at. % and 51 mm diameter) in an $Ar + O_2$ gas mixture. The target was sputtered with a constant current density J = 50 A m^{-2}. The distance between the target and the substrate was fixed at 65 mm. The gas flow rates were controlled by

a homemade system [21]. All depositions were carried out with an argon flow rate of 2 sccm and a constant pumping speed of 10 L s^{-1}, which produced an argon partial pressure of 0.28 Pa. Oxygen mass flow rate was periodically controlled versus time according to a rectangular signal by the reactive gas pulsing process, namely RGPP [22]. The pulsing period T of the oxygen flow rate was changed from 22 to 433 s to produce ten different periodic metal/oxide alternations (Ta_{pure}, Ta1 to Ta9, samples). The maximum O_2 flow rate was fixed at 1.6 sccm during the t_{on} injection time. Otherwise it was completely stopped (no oxygen injection) during the t_{off} time. The expected tantalum/tantalum oxide period Λ is in-between 5 to 100 nm, with $\Lambda = \lambda_{met} + \lambda_{ox}$, where λ_{met} and λ_{ox} are the thicknesses of the metal and oxide sub-layers, respectively. As a result, the duty cycle α defined as the ratio t_{on}/T takes values from 26 to 66% of T in order to tune the $\lambda_{ox}/\lambda_{met}$ ratio. Moreover, the deposition procedure always started with the O-rich layer and finished with the Ta-rich in order to reach a total thickness close to 260 nm.The local structure was examined by high resolution transmission electron microscopy to check the thickness, interface and local order in each sub-layer. The chemical composition was determined by energy-dispersive X-ray spectroscopy implemented in a TEM JEOL 2100 LaB_6. Moreover, dc electrical resistivity ρ of the films deposited on glass substrates was performed versus temperature from 300 to 470 K with a homemade system based on the Van der Pauw method.

3. Results and discussion

3.1 HRTEM results

The study of cross-sectional view by TEM allows the observation of distinct alternations of tantalum and tantalum oxide sub-layers for all samples. Indeed, clear interfaces of different chemical phases can be observed and measured by TEM images irrespective of the Λ period for each sample (Fig. 1a and 1b). TEM allows a nanometric measurement (± 1 nm) for total thickness (e_{tot}) and sub-nanometric (± 0.2 nm) for period and sub-layer thicknesses (Λ and λ, respectively). Measurements of total period Λ are included between 5.4 and 78.6 nm, with e_{tot} ranging from 203 to 330 nm (Fig. 1a and 1b). Dc reactive sputtering with the RGPP technique has performed sub-layer thickness lower than 2 nm as it can be observed in figure 1a by TEM analyses. Indeed, this technique allows obtaining λ_{met} included between 1.9 nm and 50.8 nm, and λ_{ox} between 3 nm and 27.8 nm, respectively.

The energy-dispersive X-ray spectroscopy analysis was used to determine the chemical composition of sub-layers of metal (dark bands) and oxide (bright bands). In the O-rich sub-layers, the amount of Ta is 27 at. % and 73 at. % for O with a variation of less than 4 % between all samples. This reveals an oxide phase of composition close to Ta_2O_5. For the Ta-rich sub-layers, the EDX measurements show that this layer is mainly composed by tantalum with 90 at. % of Ta and 10 at. % of O. The composition of the metal sub-layer does not fall below 81 at. %. So

the occurrence of two phases can be possible with some inclusions of tantalum oxide in the pure metallic sub-layer.

Association of HRTEM images and diffraction patterns allows the observation of some eventual crystalline phases. By comparing experimental and simulated (JEMS software) patterns, the determination and identification of crystals are accurately done. HRTEM pictures highlight that Ta-rich sub-layer is partially crystallized and that the O-rich layer is completely amorphous. Moreover, the systematic HRTEM study reveals that the crystallization starts for $\lambda_{met} > 10$ nm with small crystallite size about 3 – 5 nm and finishes with a quasi total crystallization for the biggest periods. Zone axes (ZA) [111] of α-Ta have been indexed for all crystallites (Fig. 1.c) with interplanar distances typical of pure Ta ($d_{111} = 2.33$ Å). Moreover, the diffraction pattern presented in figure 1.d points out the α-Ta cubic phase. TEM study allows concluding that the Ta/TaO_x multilayers deposited by dc magnetron sputtering are all composed by α-Ta/a-Ta_2O_5 for Ta-rich and O-rich sub-layers, respectively.

3.2 Conductivity measurements and discussion

Characterization of gas sensor is most often carried out by conductivity measurements varying temperature. For the gas sensor characterization, it would be ideal to measure only the electrical contribution of gas adsorbed quantity by freeing itself of the sensitive material contribution while varying the temperature. Obtain

such hybrid and invariant electrical behavior versus temperature can be interesting for gas sensor application.

Every sample has been characterized by Van der Pauw analyses with two cycles of measurements. They have been carried out for thin films grown on glass substrate to avoid the contribution of silicon conductivity. The cycle starts at room temperature, then, the substrate is heated up to 200 °C using 2 °C min^{-1} increment. A plateau of 10 min is set at 200 °C before coming back to room temperature with the same ramp of temperature. These analyses (Table 1) all exhibit a linear evolution of the electrical resistivity versus temperature with ρ_0 included between 1.77×10^{-06} and 4.10×10^{-06} Ω m.

The Ta1 sample rather exhibits a semiconducting resistivity value and behaviour with $\rho_0 = 1.82\times10^{-04}$ Ω m. All samples have a negative slope when ρ is plotted versus temperature, but two samples (Ta8 and Ta9) get a quasi constant resistivity versus temperature. In fact, they all have a metallic-like behaviour but with positive or negative temperature coefficients of resistivity according to the Λ period size (TCR = α_0 in Table 1). For metals, the variation of resistivity with temperature is a function of TCR. This latter is expressed as a percentage of resistivity variation in temperature relative to the initial value ρ_0 obtained at $T_0 = 25$ °C.

$$\rho = \rho_0\left[1+\alpha_0\left(T - T_0\right)\right] \quad (1)$$

In order to better understand the electrical properties of tantalum/tantalum oxide multilayers, we first assumed that the charge carrier concentration and mobility are high. To have an equivalent parameter in terms of structure which will be noted χ, mobility and charge carrier concentration can be brought back to the amount of metal present in the λ_{met} sub-layers under the amount of insulator in the λ_{ox} sub-layers. The χ parameter defined as $\chi = \lambda_{met}/\lambda_{ox}$, can be calculated without taking into account the metal concentration as it is a constant in all sub-layers.

Van der Pauw analyses pointed out that any samples have a positive TCR like the Ta_{pure} reference sample. Moreover, resistivity measurements highlight that the ratio χ must be higher than 3 to obtain a metallic-like behaviour with a quasi zero TCR value. By studying the data provided in table 1, no clear dependence between the values of Λ, λ_{met}, λ_{ox}, and ρ can be pointed out. Only the structural parameter χ may explain the change of electrical response. Indeed, when χ increases, ρ decreases to tend towards the behaviour of the Ta_{pure} reference sample. The insertion of the χ parameter is therefore crucial to understand the relationship of interdependence between electrical properties and structural of multilayered thin films.

4. Conclusion

Dc reactive sputtering deposition of tantalum and tantalum oxide periodic nanometric multilayers was successful with the reactive gas pulsing process. The transmission electron microscope study showed sharp interfaces between the sub-layers. EDX and TEM analyses proved that the Ta-rich sub-layers was composed

by crystalline α-Ta for $\lambda_{met} > 10$ nm, whereas the O-rich sub-layers are composed by amorphous a-Ta_2O_5. The study of the electrical properties was carried out by Van der Pauw method, pointing out a metallic behaviour for $\lambda_{met} > 1.9$ nm. Sub-layers thickness and composition were accurately determined by TEM introducing the χ parameter, which allows explaining the electrical behaviour. The interdependence relationship was demonstrated between the electrical properties and the structure of thin α-Ta/aTa_2O_5 periodic multilayers.

References

[1] S. Duenas, E. Castan, J. Barbolla, R.R. Kola, P.A. Sullivan, *Journal of Materials Science: Materials in Electronics.* 10 **(**1999) 379-384.

[2] R.K. Krishnan, K.G. Gopchandran, V.P. Mahadevanpillai, V. Ganesan, V. Sathe, Applied Surface Science, 255 (2009) 7126-7135.

[3] C. Grivas, R.W. Eason, Journal of Physics – Condensed Matter, 20 (2008) 264011.

[4] A.J. Waldorf, J.A. Dobrowski, B.T. Sullivan, L.M. Plante, Applied Optics 32 (1993) 5583.

[5] C.T. Wu, F.H. Ko, C.H. Lin, Applied Physics Letters, 90 (2007) 171911.

[6] R. Rabady, I. Avrutsky, Applied Optics, 44 (2005) 378-383.

[7] E. Atanassova, D. Spassov, A. Paskaleva, M. Georgieva, J. Koprinarova, Thin Solid films, 516 (2008) 8684-8692.

[8] N. Novkovski, E. Atanassova, Applied Physics Letters, 86 (2005) 152104.

[9] P.C. Joshi, M.W. Cole, Journal of Applied Physics, 86 (1999) 871.

[10] S.H. Yang, Y.Y. Liu, G.Z. Qiu, M.T. Tang, Rare Metal Materials and Engineering, 36 (2007) 2075-2079.

[11] W.X. Zeng, E. Eisenbraun, H. Frisch, J.J. Sullivan, A.E. Kaloyeros, J. Margalit, K. Beck, Journal of the electrochemical society, 151 (2004) F172-F177.

[12] A. Porporati, S. Roitti, O. Sbaizero, Journal of the European Ceramic Society, 23 (2003) 247-251.

[13] Y.H. Pai, C.C. Chou, F.S. Shieu, Materials Chemistry and Physics, 107 (2008) 524-527.

[14] C.C. Lee, D.J. Jan, Thin Solid films, 483 (2005) 130-135.

[15] A. Paskaleva, E. Atanassova, T. Dimitrova, Vacuum, 58 (2000) 470-477.

[16] H.E. Cheng, C.T. Mao, Japanese Journal of Applied Physics, 45 (2006) 160.

[17] A. Cacucci,V. Potin, L. Imhoff, M.C.M. de Lucas, N. Martin, *Thin Solid Films,* **520 (**2012) 4778-4781.

[18] S. Berg, H.O. Blom, T. Larsson, C. Nender, Journal of Vacuum Science and Technology, A5 (1987) 202.

[19] W.D. Sproul, D.J. Christie, D.C. Carter, Thin Solid Films, 491 (2005) 1-2.

[20] R.P. Howson, Pure Applied Chemistry, 66 (1994) 1311-1318.

[21] J.M. Chappé, N. Martin, J. Lintymer, F. Sthal, G. Terwagne and J. Takadoum*, Applied Surface Science*, 253 (2007) 5312-5316.

[22] N. Martin, J. Lintymer, J. Gavoille, J.M. Chappé, F. Sthal, J. Takadoum, et al, *Surface and Coatings Technology*, 201 (2007) 7720-7726

Tables

Table 1

Structural parameters and resistivity results from Van der Pauw analyses for Ta1 to Ta9 with Ta_{pure} as reference sample.

name of sample	e_{tot} *(± 2 nm)*	Λ *(± 0,1 nm)*	λ_{met} *(± 0,1 nm)*	λ_{ox} *(± 0,1 nm)*	χ *(± 0.05)*	ρ_0 *(Ω m)*	α_0 *(K^{-1})*	$\rho_{(470K)}$ *(Ω m)*
Ta1	330	5,4	1,9	3,5	0,54	$1,82\times10^{-04}$	$-2,62\times10^{-03}$	$9,84\times10^{-05}$
Ta2	278	5,6	2,6	3	0,87	$4,12\times10^{-06}$	$-2,36\times10^{-04}$	$3,95\times10^{-06}$
Ta3	264	8	4,3	3,7	1,16	$3,25\times10^{-06}$	$-2,11\times10^{-04}$	$3,13\times10^{-06}$
Ta4	244	9,8	5,8	4	1,45	$2,90\times10^{-06}$	$-4,93\times10^{-04}$	$2,65\times10^{-06}$
Ta5	239	14,7	9,3	5,4	1,72	$2,80\times10^{-06}$	$-9,39\times10^{-04}$	$2,34\times10^{-06}$
Ta6	237	78,6	50,8	27,8	1,83	$2,60\times10^{-06}$	$-3,30\times10^{-04}$	$2,45\times10^{-06}$
Ta7	220	20,2	13,7	6,5	2,11	$2,23\times10^{-06}$	$-5,12\times10^{-04}$	$2,03\times10^{-06}$
Ta8	272	16	12	4	3,00	$1,87\times10^{-06}$	$-1,53\times10^{-04}$	$1,82\times10^{-06}$
Ta9	272	45.3	35,3	10	3,53	$1,76\times10^{-06}$	$-1,94\times10^{-04}$	$1,71\times10^{-06}$
T_{pure}	300	-	-	-	-	$1,90\times10^{-07}$	$1,20\times10^{-03}$	$2,30\times10^{-07}$

Figure Captions

Figure 1

Cross section TEM image of a) Ta1 and b) Ta6 samples, c) HRTEM picture of α-Ta ZA [111] in Ta7 sample, and d) diffraction pattern of Ta5 deposit with d_{111} surrounded.

a) Cross section TEM image of Ta1 sample

b) Cross section TEM image of Ta6 samples

c) HRTEM picture of α-Ta ZA [111] in Ta7 sample

d) Diffraction pattern of Ta5 deposit with d_{111} surrounded.

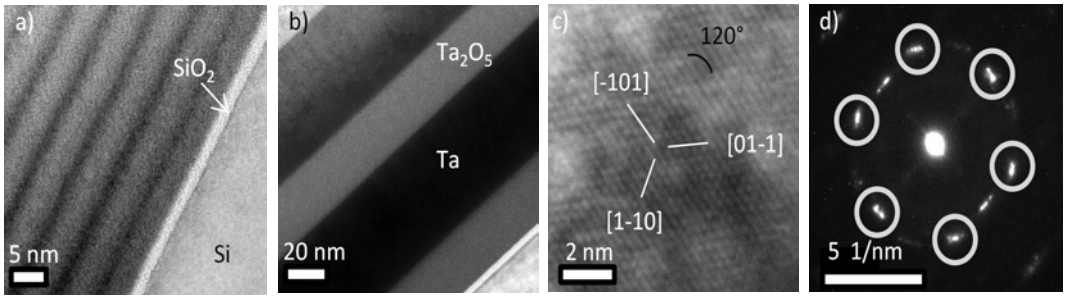

Figure 1